JOC The Journal of Organic Chemistry

Article

Synthesis of Chiral Alkenyl Cyclopropane Amino Acids for Incorporation into Stapled Peptides

Tsz Ying Yuen, Christopher J. Brown, Yaw Sing Tan, and Charles William Johannes

J. Org. Chem., **Just Accepted Manuscript** • Publication Date (Web): 11 Dec 2019

Just Accepted

is published by the American Chemical Society. 1155 Sixteenth Street N.W., Washington, DC 20036

Synthesis of Chiral Alkenyl Cyclopropane Amino Acids for Incorporation into Stapled Peptides

Tsz Ying Yuen*[a], Christopher J. Brown[b], Yaw Sing Tan,[c] and Charles W. Johannes[b]

[a]Institute of Chemical and Engineering Sciences, Agency for Science, Technology and Research, 8 Biomedical Grove, Neuros, #07-01, Singapore 138665

[b]P53 Laboratory, Agency for Science, Technology and Research, 8A Biomedical Grove, #06-06, Immunos, Singapore 138648

[c]Bioinformatics Institute, Agency for Science, Technology and Research, 30 Biopolis Street, #07-01, Matrix, Singapore 138671

Abstract

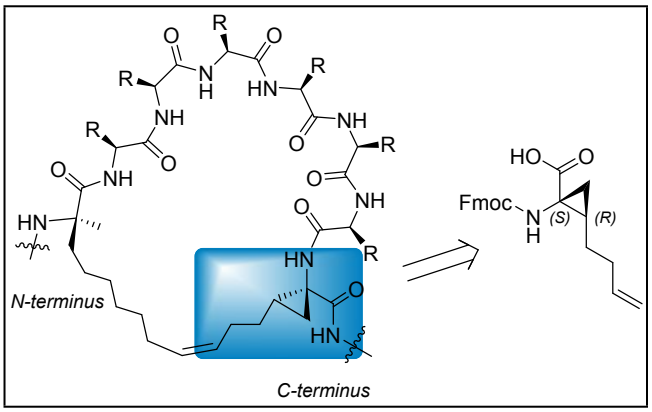

α,α'-Disubstituted amino acids serve as important non-proteinogenic amino acids in the construction of stabilised helical peptides. To expand the repertoire of α,α'-disubstituted amino acids, chiral alkenyl-containing cyclopropane amino acids were synthesised via a two-step olefination and cyclopropanation procedure. Herein we report the first example of the use of alkenyl cyclopropane building blocks to constrain MDM2-targeting helical peptides. The increased potency and efficacy associated with C-terminal cyclopropane substitution is postulated to be driven by a combined effect of net hydrophobicity and enhanced protein association rates.

Introduction

Protein-protein interfaces (PPI) represent a promising class of targets for therapeutic development.[1] In cancer, PPIs form signalling nodes that transmit oncogenic signals along molecular networks, promoting tumour progression and metastasis.[2, 3] Among the tumour suppressor genes, p53 is arguably one of the most studied.[4-8] It is a key transcription factor that activates genes responsible for DNA repair in response to cellular stress. Additionally, p53 induces the expression of MDM2, which promotes p53 degradation, forming an autoregulatory feedback loop. More than 50% of human tumours carry p53 mutations and another 17% exhibit overexpression of MDM2.[9] Thus the p53-MDM2 pathway is a prime target for new cancer drug development.

Whilst small molecule inhibitors have had some success in targeting PPIs, they generally lack the specificity and potency to address complex PPIs with extended or flat surfaces.[10-13] Stabilised α-helical peptides on the other hand are increasingly being considered for the modulation of these challenging PPIs, in part due to their ability to mimic secondary epitopes that make up ~60% of PPIs.[14, 15] The first all-hydrocarbon stapled peptides have already entered clinical trials targeting MDM2-amplified and p53-mutant tumour cells.[16-18] Promising results have served to validate the potential of this therapeutic approach for treating human diseases.

Hydrocarbon stapled peptides are a class of helix mimetics derived from the cross-linkage of two alkenyl amino acids of the same peptide. Pioneered by Grubbs and co-workers,[19-21] the methodology

was further extended by Verdine through the introduction of α,α'-disubstituted amino acids.[22] To date, a number of hydrocarbon staples have been described that encompass one or two helical turns.[23-28] Analogues with two staples spanning different stretches of the peptide (double stapled peptides[29-32]) or sharing a central spiro junction (stitched peptides[33]) have also been reported. However, the underlying design principle remains the same: incorporation of α,α'-disubstituted alkenyl amino acids imposes unfavourable steric interactions between the peptide backbone and the β-substituents, reducing backbone flexibility.[34-37] In an organic environment, the peptide exhibits partial helicity, achieving an optimal orientation for macrocyclisation to occur. Introduction of strategically placed covalent constraints along the peptide reduces conformational entropy and may indirectly contribute to a number of pharmacologic advantages such as enhanced target engagement, extended *in vivo* half-life and cell penetration through active transport.[25, 27, 38, 39]

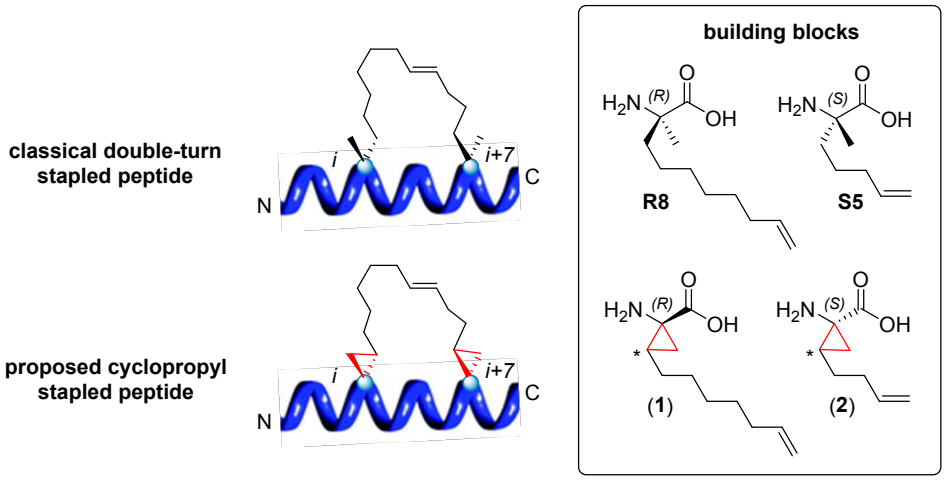

Figure 1. Building blocks of all-hydrocarbon stapled peptide.

Except for the C=C bond, all other carbon-carbon bonds of the staple are free to rotate and can adopt multiple conformations. A study on a related cysteine-bridged α-helical peptide has recently shown that maximal stabilisation could be achieved using rigid cross-linkers.[40] From this standpoint, it may be desirable to further restrain the all-hydrocarbon linker. The cyclopropane moiety has been extensively used in medicinal chemistry for restricting the conformation of small molecules.[41-44] By tying together the β-carbons of the staple into a cyclopropane ring, we anticipate further stabilisation of the bioactive peptide conformation with minimal change to the overall structural conformation (Figure 1). The configuration of the α-stereocenter (*R* or *S*) of cyclopropane amino acids **1** and **2** was designed to be consistent with the α-methyl systems (R8 and S5) used for the classical double-turn stapled peptides.

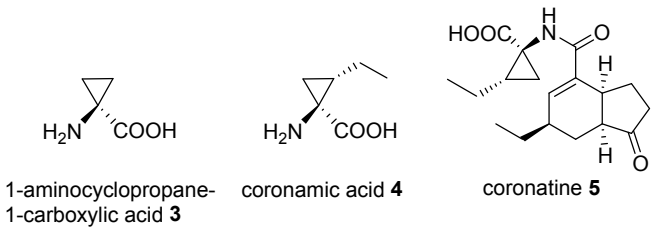

Figure 2. Examples of naturally occurring cyclopropane amino acids.

1-aminocyclopropane-1-carboxylic acid (ACC) derivatives are naturally occurring (Figure 2). Representative examples include **3** which is present in higher plants as the ethylene precursor and coronamic acid (**4**) which functions as an intermediate in the biosynthesis of the bacterium-producing phytotoxin coronatine **5**.[45-49] Although cyclopropane amino acids have demonstrated their utility as conformationally restricting subunits in the construction of peptidomimetics,[50-54] they have not been explored in the context of constraining helical peptides. The vinyl ACC **(6)** is a particularly important structural motif for a number of hepatitis C protease inhibitors.[55-57] Its industrial preparation largely relies on the bis-alkylation of a malonate or an imine precursor (Scheme 1), where optically pure material can be obtained either via dynamic enzymatic resolution of the racemic mixture (route I)[58, 59] or direct reaction with the chiral pool material derived from butane-1,2,4-triol (route II)[60]. Asymmetric routes employing chiral catalysts or auxiliaries have also been described (routes III and IV)[61-64].

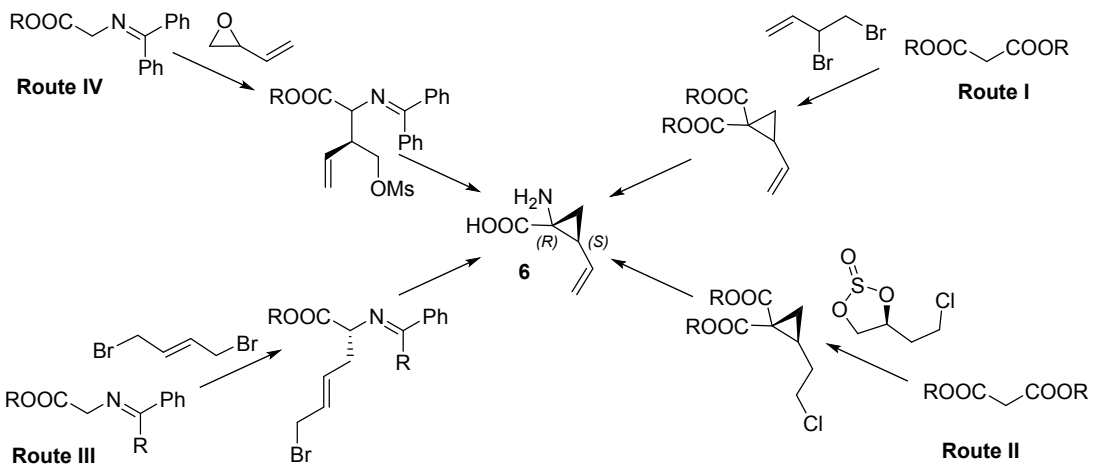

Scheme 1. Synthetic routes to vinyl cyclopropane amino acid **6**.

In general, absolute stereocontrol of the substituents around the cyclopropane ring provides a significant challenge. Whilst a number of strategies have been developed based on the manipulation of iodonium ylides or diazo compounds,[65-69] we favoured the more chemically flexible method of using chiral didehydro derivatives as an entry to ACC's **1** and **2** (Scheme 2).[70, 71] The synthetic strategy involved the cyclopropanation of a didehydro derivative (**7**), formed by olefination of a chiral glycine template (**8**) with an alkenyl aldehyde precursor (**9**). The stereochemistry at the *β*-position of the ACC's can be controlled in a highly selective fashion, simply by appropriate choice of the olefination conditions. Reaction of aldehyde **9** under Horner-Wadsworth-Emmons conditions[72-75] should provide *E*-(**7**) whereas direct condensation of **8** with **9** under strong basic conditions should lead to the *Z* isomer.[76-78] For this proof of concept study, we focused only on the latter strategy. More importantly, the C-6 substituent of oxazinone **8** serves to block one face of the heterocycle so that ensuing cyclopropanation becomes stereoselective. Deliberate choice of the isopropyl stereochemistry should enable access to both *(1R,2S)*- and *(1S,2R)*-ACC's.

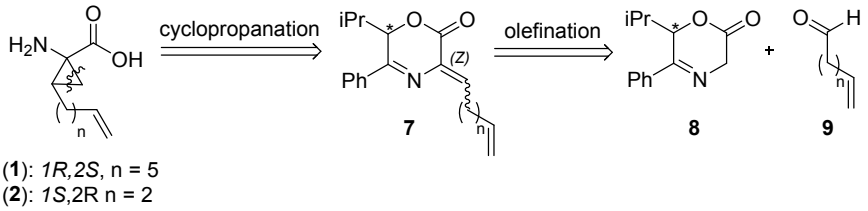

Scheme 2. Retrosynthetic analysis for the synthesis of cyclopropane ACC's via cyclopropanation.

Results and Discussions

Chiral glycine template **8** was prepared from *(S)*-2-hydroxyisovaleric acid (Scheme 3). According to a reported method,[70] **10** was converted to an amide before undergoing a Grignard reaction and coupling with Boc-glycine to afford ester **12**. Following Boc deprotection, addition of excess base resulted in the formation of *(S)*-**8** along with hydrolysed intermediate **11**. By limiting the amount of base added to exactly one equivalent, the desired oxazinone could be obtained in good yield without hydrolysis.

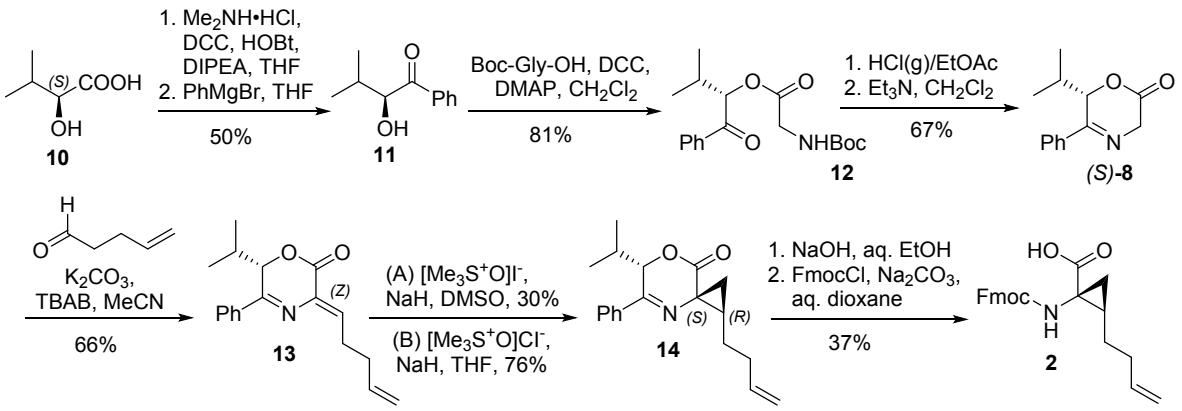

Scheme 3. Synthesis of *(1S,2R)*-ACC **2**.

Reaction of *(S)*-**8** with pent-4-enal in the presence of potassium carbonate and tetrabutylammonium bromide furnished intermediate **13** as a single stereoisomer in 66% yield after column chromatography. The relative stereochemical configuration was inferred from ^{1}H NMR spectroscopy. Compared to the terminal olefin protons, the C-H peak of the α,β-unsaturated alkene appeared further downfield at 6.91 ppm with a vicinal coupling constant of 8.0 Hz, indicating the desired *Z*-isomer had been formed.[77] Moreover, as we did not prepare racemic standards, our assignment of reaction selectivity, and the presumption of absolute stereochemistry relies on analogy to the literature precedent, which appears consistent with our preparation of the alternative isomers of the peptides, as exemplified below.

Treatment of **13** with Corey's dimethylsulfoxonium methylide,[79] prepared by the deprotonation of trimethylsulfoxonium iodide with sodium hydride in DMSO (condition A) afforded the cyclopropane derivative **14** in a low 30% yield. Although unreacted **13** could be recovered and subjected to another round of reaction, we had found the iodide-derived ylide to be unstable. On the other hand, when trimethylsulfoxonium chloride was used in THF (condition B), we successfully obtained **14** as a single diastereoisomer (unreacted **13** had eluted together with **14**, but a minor isomer was not observed by ^{1}H NMR). Given that the cyclopropanation reaction should occur *anti* to the isopropyl group from the

less-hindered face, **14** was expected to possess the desired (*S*,*R)*-stereochemistry. Subsequent hydrolysis and Fmoc protection afforded ACC **2**.

Using a similar strategy, *(R)*-**8** was assembled from *(R)*-2-hydroxyisovaleric acid in 29% yield over 5 steps (Scheme 4). Oct-7-enal **18** was synthesised from the corresponding alcohol.[80] Since it was not very stable, **18** was prepared fresh and used immediately in the next step without further purification. Compared to the earlier olefination attempt using pent-4-enal (Scheme 3), **18** was less reactive and led to the recovery of significant amounts of unreacted starting material after overnight reaction. Extensive screening of alternative bases did not improve the yield but complete conversion of starting *(R)*-**8** to **19** was finally achieved when stoichiometric amounts of the phase-transfer catalyst were used in dichloromethane. A triplet at 6.93 ppm with a coupling constant of 8.0 Hz confirmed the formation of the desired *Z*-isomer. Cyclopropanation using the previously established protocol afforded **20** as a single stereoisomer which was converted to *(1R,2S)*-ACC **1** via a two-step auxiliary cleavage and Fmoc protection protocol.

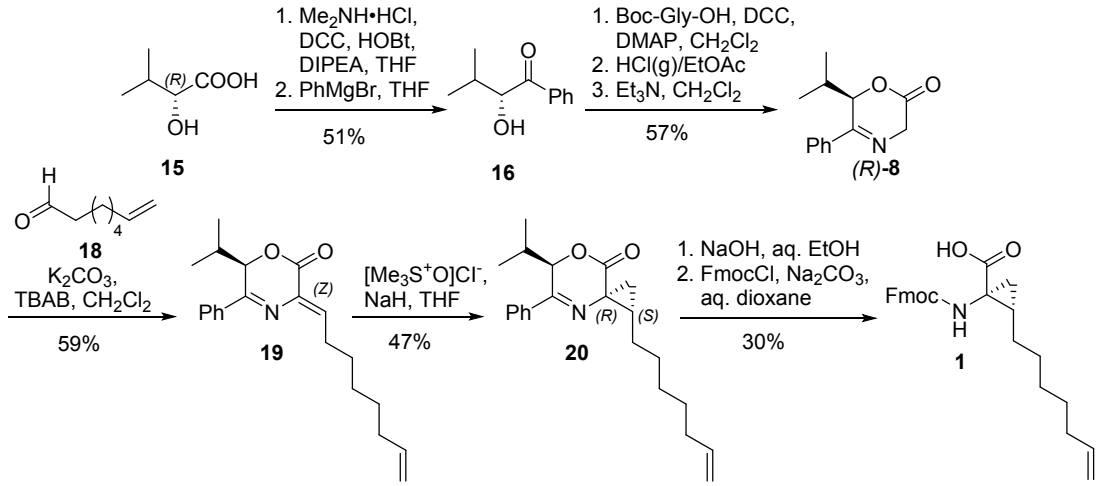

Scheme 4. Synthesis of *(1R,2S)*-ACC **1**.

To determine whether the introduction of tether rigidity would further enhance the binding affinity and biological activities of stapled peptides, conformationally constrained analogues were prepared. VIP116 and sMTide-02 were chosen as model peptides as they had previously been shown to restore p53 function via disruption of the p53/MDM2 complex.[23, 81, 82] ACC's **1** and **2** were introduced as either single or double replacements for the conventional stapling building blocks (Table 1).

Whilst all linear peptide precursors were successfully synthesised, the key macrocyclisation step had failed when two cyclopropane groups were present in the peptide sequence (entries 3 and 7). *A priori* this was unexpected, and to further understand this new system we evaluated other combinations of the ACC's with known α-methyl stapling building blocks. ACC **2** was tolerated well in both peptide templates (entries 4 and 8) in combination with R8. VIP116 with the ACC **1** and S5 substitutions did not undergo metathesis to any measurable extent (entry 5) but elongation of the tether by one methylene group resulted in the formation of cyclic peptide VIP145 (entry 6). In the case of sMTide-02, macrocyclisation proceeded smoothly in the presence of ACC **1**, with or without tether extension (entries 9-10). However compared to the 34-membered cyclic peptide VIP143, formation of the smaller, 33-membered VIP142 was less clean and a final purity of >90% could not be achieved by HPLC.

The different reactivity profiles for macrocyclisation suggested we should also expect different binding effects to MDM2.

Entry	Peptide	Sequence	K_d (nM)
1	VIP116	Ac-Lys-Ahx-Thr-Ser-Phe-(R8-Glu-Tyr-Trp-Ala-Leu-Leu-S5)-Glu-Asn-Phe-NH_2	12.5 ± 0.3
2	sMTide-02	Ac-Thr-Ser-Phe-(R8-Glu-Tyr-Trp-Ala-Leu-Leu-S5)-NH_2	34.4 ± 2.0
		Cyclopropane-substituted VIP116	
3	-	Ac-Lys-Ahx-Thr-Ser-Phe-(**1**-Glu-Tyr-Trp-Ala-Leu-Leu-**2**)-Glu-Asn-Phe-NH_2	N/A
4	VIP144	Ac-Lys-Ahx-Thr-Ser-Phe-(R8-Glu-Tyr-Trp-Ala-Leu-Leu-**2**)-Glu-Asn-Phe-NH_2	5.4 ± 0.5
5	-	Ac-Lys-Ahx-Thr-Ser-Phe-(**1**-Glu-Tyr-Trp-Ala-Leu-Leu-S5)-Glu-Asn-Phe-NH_2	N/A
6	VIP145	Ac-Lys-Ahx-Thr-Ser-Phe-(**1**-Glu-Tyr-Trp-Ala-Leu-Leu-**S6**)-Glu-Asn-Phe-NH_2	40.0 ± 3.0
		Cyclopropane-substituted sMTide-02	
7	-	Ac-Thr-Ser-Phe-(**1**-Glu-Tyr-Trp-Ala-Leu-Leu-**2**)-NH_2	N/A
8	VIP141	Ac-Thr-Ser-Phe-(R8-Glu-Tyr-Trp-Ala-Leu-Leu-**2**)-NH_2	4.7 ± 1.0
9	VIP142	Ac-Thr-Ser-Phe-(**1**-Glu-Tyr-Trp-Ala-Leu-Leu-S5)-NH_2	150.0 ± 14.9
10	VIP143	Ac-Thr-Ser-Phe-(**1**-Glu-Tyr-Trp-Ala-Leu-Leu-**S6**)-NH_2	172.1 ± 14.0

Table 1. K_d values of cyclopropane-fused analogues of sMTide-02 and VIP116, determined by competitive fluorescence anisotropy titrations

Except for VIP141 and VIP144, all other peptides eluted as two peaks by chromatography. Both peaks had identical masses and were assumed to be the *E*- and *Z*- isomers. From experience, separation of closely eluting stapled peptides by reversed-phase HPLC can be particularly difficult, with each additional round of purification leading to substantial loss of material. Therefore all peptides were tested as mixtures without further isomer separation. MDM2 binding affinity of the peptides was determined using a competitive fluorescence anisotropy assay.[83] In general, single ACC **2** substitution at the *i+7* position increased binding potency (entries 4 and 8) whereas incorporation of ACC **1** at the *i* position led to higher K_d values (entries 6, 9-10). These results, coupled with earlier experimental observations, suggest (*1R,2S*)-ACC **1** may not be correctly mimicking the bound conformation of the parent stapled peptide and that the alternative *(1R,2R)*-configuration should be pursued.

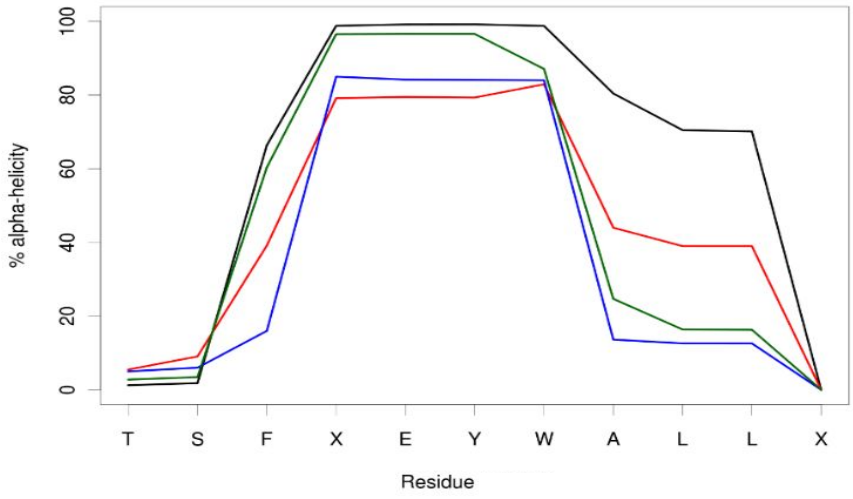

Figure 3. α-helix propensity of residues in sMTide-02 (black), VIP141 (green), VIP142 (red) and dicyclopropane-substituted sMtide-02 (blue).

Molecular dynamics (MD) simulations of the unbound stapled peptide and MDM2-peptide complexes were performed to explain the binding affinity trend observed in the FP assay. The shorter peptide sMTide-02 was chosen as the template to minimise variations in energies due to transient interactions of the flexible peptide regions with MDM2. The results showed no significant variation between the computed binding enthalpies of sMTide-02 and the cyclopropane-constrained stapled peptides (Table 2). There was, however, a marked difference in the α-helicities of the unbound peptides (Figure 3), suggesting the observed binding affinity discrepancy was due to entropic factors. The most helical peptide was sMTide-02, followed by VIP141, VIP142 and dicylopropane-substituted sMTide-02, which saw a loss in helicity throughout its entire length. Substitution of R8 with its cyclopropyl analogue had led to a loss in helicity at the N-terminal end of the peptide, whereas substitution of S5 with its cyclopropyl analogue resulted in a loss of helicity at the C-terminal end. As a result, dicyclopropane-substituted sMTide-02 has the lowest overall α-helicity and likely incurs the highest entropy penalty upon binding to MDM2.

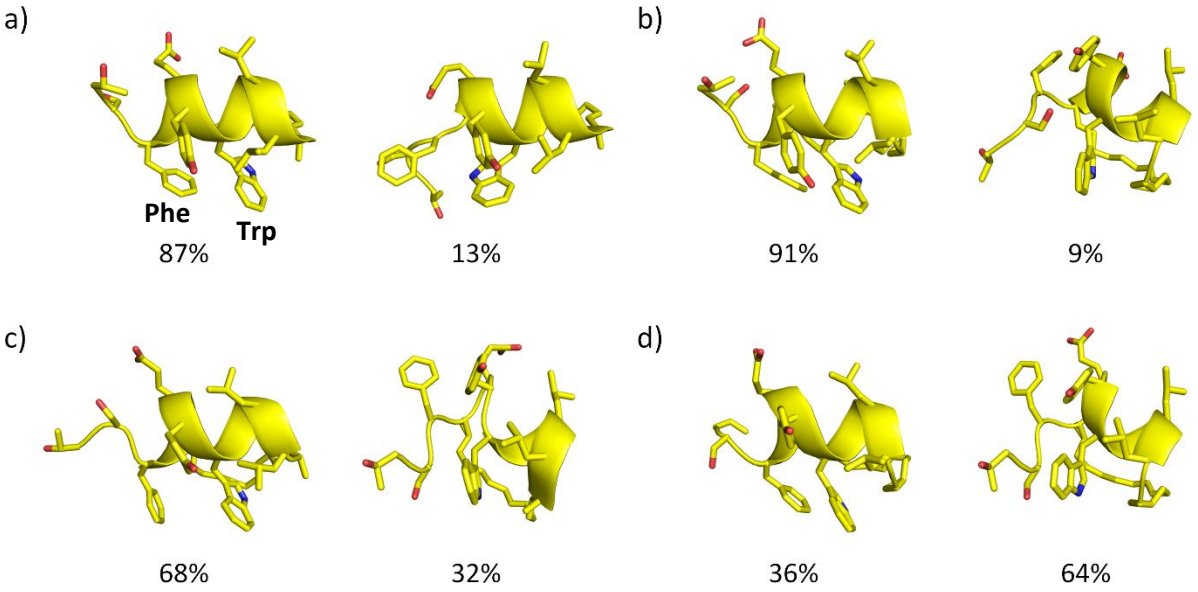

Figure 4. MD trajectory structures with lowest root-mean-square-deviation (RMSD) from cluster centroids of (a) sMTide-02, (b) VIP141, (c) VIP142, and (d) dicyclopropane-substituted sMTide-02. Percentage populations of each cluster are indicated.

Enhanced helical stability is often a consequence of hydrocarbon stapling, however this alone does not guarantee optimal biochemical or biological activity.[84] Contrary to the α-helicity trend, VIP141 exhibited a higher affinity for MDM2 than the more helical sMTide-02. To explain this inconsistency, conformations derived from the MD simulations of the free peptides were clustered. It can be seen that all stapled peptides had adopted two major conformations: one with the N-terminal end folded into a helix and the key binding residues Phe and Trp aligned along the same plane, and another with the N-terminal end unfolded and Phe and Trp misaligned (Figure 4). There is evidence to show that MDM2 initially binds Phe, followed by Trp, and finally the rest of the peptide.[85, 86] Hence, peptide

conformations with Phe and Trp aligned in the same plane would be able to associate faster with MDM2. VIP141 was found to have the highest proportion of conformations with Phe and Trp aligned (91%), whilst sMTide-02 showed a slightly lower value of 87%. Hence VIP141 is likely to have a faster association rate and higher binding affinity for MDM2. The simulations also show that substitution of R8 with its cyclopropyl analogue in VIP142 leads to a significant loss of helicity at its N-terminal end, thus reducing the proportion of conformations with aligned Phe and Trp (68%). This could explain why although VIP142 is predicted to have comparable α-helicity with VIP141, it exhibited weaker binding to MDM2.

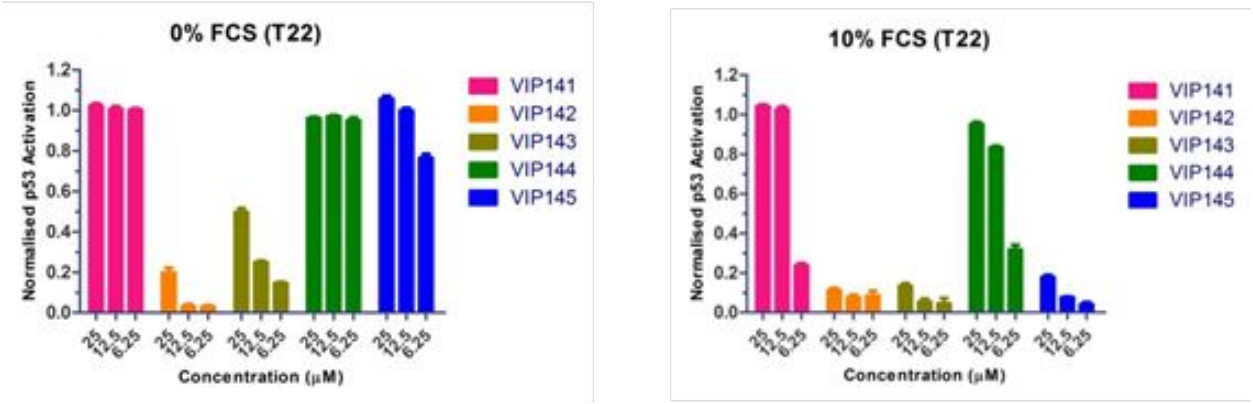

Figure 5. p53 transcriptional activity of VIP141-145. Normalisation of measurements was performed by setting the readings taken from cells treated with DMSO and sMTIDE-02 (25 μM at 0% FCS) to 0 and 1, respectively.

Serum binding is a common property of stapled peptides and sMTide-02 is no exception.[23] Using a cell-based p53 reporter assay, the EC_{50} values of sMTide-02 (*E/Z* mixture) were previously determined to be 3.5 ± 0.3 μM and 18.2 ± 0.7 μM in 0% and 10% serum, respectively.[81] VIP141-145 were screened at three different concentrations, with or without fetal calf serum (FCS), and their p53 transcriptional activities were normalised against the maximum cellular activity induced by sMTide-02 at 25 μM in the absence of serum.

As seen from Figure 5, the most potent cyclopropane-constrained peptides induced the highest levels of p53 activation in the absence of serum. Not only did VIP141 and 144 exhibit similar p53 activation levels (normalised value of 1) to that of the control at all concentrations tested, the peptides appeared to be less affected by serum components. This was evident by the maintained cellular activity (normalised values >0.8 at 25 and 12.5 μM) in the presence of 10% FCS. Although VIP145 also caused similar levels of p53 induction in the absence of serum, a significant drop in p53 activity was observed when the assay was repeated under the more physiologically relevant conditions.

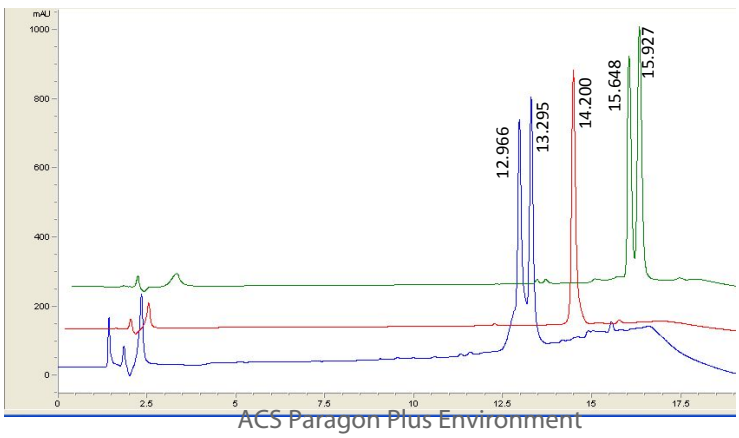

Figure 6. RP-HPLC spectra of sMTide-02 (green), VIP141 (red) and VIP142 (blue).

HPLC retention time has been shown to correlate with apparent hydrophobicity and is used as the hydrophobicity determinant for a number of studies involving peptides.[87-90] Despite having identical net charge, %helicity and hydrocarbon content, differences in the apparent hydrophobicity could be observed between VIP141 and VIP142 where the more hydrophobic VIP141 was found to be more bioactive. Likewise, although VIP142 and VIP143 exhibited comparable K_d values (Table 1), the more hydrophobic VIP143 was more effective at inducing p53 activation at 0% FCS (Figure 5 and SI). These results further lend support to previous hypothesis that increased hydrophobicity leads to enhanced stapled peptide permeability and cellular activity.[82, 91, 92]

Peptide	HPLC retention time (min)	α-helicity (%)	ΔH (kcal/mol)
sMTide-02	15.79	62.4	-58.2 ± 1.0
VIP141	14.20	45.5	-59.1 ± 0.4
VIP142	13.13	45.1	-58.5 ± 1.2
Dicyclopropane-substituted sMTide-02	NA	36.7	-59.3 ± 1.5

Table 2. Apparent hydrophobicity (as expressed by the average RP-HPLC retention times of the *E/Z* isomers), α-helicity (calculated by averaging the helix propensity of each residue) and binding enthalpies of sMtide-02, VIP141, VIP142 and dicyclopropane-substituted sMTide-02.

Conclusions

In summary, a general method for the preparation of Fmoc-protected alkenyl 1-aminocyclopropane-1-carboxylic acid building blocks was described. Base-mediated olefination of a chiral oxazinone provided the necessary *Z*-didehydro template for the key asymmetric cyclopropanation. This synthetic strategy is amenable to a range of aldehydes with varying alkenyl chain lengths. Access to the corresponding *E*-didehydro derivative is currently underway in our laboratory for further evaluation.

ACC's **1** and **2** represent novel chiral amino acid building blocks and their utility has been demonstrated in the preparation of constrained stapled peptides. Whist introduction of the cyclopropyl groups did not further reinforce the alpha-helicity of stapled peptides targeting the p53/MDM2 protein-protein interaction, replacement of the conventional S5 building block with ACC **2** was found to enhance peptide potency and activity. More significantly, VIP141 and VIP144 were not serum sensitive at 25 and 12.5 μM. This work expands the available chemical space to explore non-proteinogenic effects with peptide macrocycles and should serve as useful templates for the chemical community.

Experimental Section

General Method. All reagents and solvents were purchased from commercial suppliers and used without further purification. All moisture and air-sensitive reactions were performed under a nitrogen or argon atmosphere using oven-dried glassware with magnetic stirring. IKA RCT basic type heating

mantle was used to provide a constant heat source. ^{1}H NMR spectra were recorded on a 400 MHz spectrometer with respect to tetramethylsilane as an internal standard. The chemical shifts are reported in δ ppm and the coupling constants (*J*) are reported in Hertz. The splitting of resonance peaks are indicated as singlet (s), doublet (d), triplet (t), quartet (q), and multiplet (m). High-resolution mass spectra (HRMS) were obtained using an electrospray ionisation (ESI) technique and a TOF mass analyser. Melting points were determined on an electrothermal melting point apparatus and are uncorrected. Compound purity was determined using two different HPLC analysis methods and the lower of the two values was taken as the result. In one method, the final cyclopropane building blocks were injected into a X-Select CSH C18 column (3.5 µm, 150 x 4.6 mm). The eluents used were 0.1% aqueous formic acid and 0.1% formic acid in acetonitrile. In another method, the ACC's were injected into a chiral YMC CHIRALART Cellulose-SC column (5 µm, 250 x 4.6 mm). The eluents used were 0.1% TFA in *n*-hexane and 0.1% TFA in a mixture of EtOH and IPA (85:15). The peptides were synthesised manually using solid phase and Fmoc chemistry using H-Ramage-Chemmatrix® resin (0.53 mmol g^{-1}). The peptides were purified by reverse-phase HPLC using an Agilent 1260 Infinity system fitted with a Phenomenex® analytical column (Jupiter C12, 4 µm, Proteo 90 Å, 150 x 4.6 mm). The eluents used were 0.1% aqueous TFA and 0.1% TFA in acetonitrile. The purified samples were assessed by HPLC-MS using a Waters 3100 single quadrupole mass detector fitted with a union. The reported MS data is for the *E/Z* peptide mixture.

(1*S*,2*R*)-1-((((9*H*-Fluoren-9-yl)methoxy)carbonyl)amino)-2-(but-3-en-1-yl)cyclopropane-1-carboxylic acid (2). To a stirred solution of (*S*)-**8**[70] (8 g, 36.86 mmol) in ACN (80 mL) at 0 °C was added K_2CO_3 (15.26 g, 110.59 mmol) followed by tetrabutylammonium bromide (2.3 g, 7.37 mmol) and stirred for 15 min. To this solution, pent-4-enal (4.02 g, 47.92 mmol) was added dropwise at 0 °C and the resulting reaction mixture was stirred at room temperature for 2 h. The reaction mixture was filtered through a pad of Celite® and the filtrate was concentrated *in vacuo*. Purification by flash column chromatography eluting with 0-10% EtOAc in *n*-hexane afforded compound **13** as a thick, colourless oil (7 g, 66%): ^{1}H NMR (400 MHz, $CDCl_3$) δ 7.85 (d, *J* = 7.2 Hz, 2H), 7.52-7.45 (m, 3H), 6.91 (t, *J* = 8.0 Hz, 1H), 5.85 (m, 1H), 5.55 (m, 1H), 5.09 (d, *J* = 16.8 Hz, 1H), 5.01 (d, *J* = 10.4 Hz, 1H), 2.79 (q, *J* = 6.8 Hz, 2H), 2.32-2.29 (m, 2H), 2.21-2.17 (m, 1H), 1.12 (d, *J* = 6.8 Hz, 3H), 0.80 (d, *J* = 6.8Hz, 3H); LCMS (ESI) m/z: $[M + H]^+$ Calcd for $C_{18}H_{22}NO_2$ 284.17; Found 284.20.

To a suspension of trimethyl sulfoxonium chloride (4 g, 14.08 mmol) and NaH (1.01 g, 42.25 mmol) at 0 °C, was added dry THF (180 mL) and the resulting reaction mixture was refluxed at 100 °C for 16 h. The reaction mixture was cooled to room temperature and the suspended solution was added to a cooled solution of **13** (4 g, 14.08 mmol) in THF (40 mL) *via* cannula. The reaction was stirred at 0 °C for 1 h then at room temperature for another hour. Progress of the reaction was monitored by TLC. After completion, the reaction mixture was concentrated *in vacuo* and purified by flash column chromatography eluting with 0-10% EtOAc in *n*-hexane to afford **14** as an off-white solid (3.2 g, 76%): ^{1}H NMR (400 MHz, $CDCl_3$) δ 7.65 (dd, *J* = 8.0, 1.6 Hz, 2H), 7.45-7.42 (m, 3H), 5.91-5.83 (m, 1H), 5.62 (d, *J* = 2.8 Hz, 1H), 5.07 (dd, *J* = 17.2, 1.2 Hz, 1H), 5.01 (d, *J* = 10.0 Hz, 1H), 2.24 (q, *J* = 6.8 Hz, 2H), 2.17-2.11 (m, 3H), 1.86-1.77 (m, 2H), 1.47 (d, *J* = 4.0 Hz, 1H), 1.12 (d, *J* = 6.8 Hz, 3H), 0.87 (d, *J* = 6.8 Hz, 3H); LCMS (MSI) m/z: $[M + H_3O]^+$ Calcd for $C_{19}H_{26}NO_3$ 316.19; Found 315.95. The compound was directly used in the next step without further characterisation as trace amounts of unreacted starting material was also detected.

Aqueous NaOH (2.15 g, 53.69 mmol in 48 mL water) was added to a solution of **14** (3.2 g, 10.74 mmol) in EtOH (48 mL). The reaction mixture was stirred at room temperature for 48 h before the solvent was removed *in vacuo*. The crude material was re-dissolved in a mixture of THF and water (1:1, 96 mL) and cooled to 0 °C before the addition of Fmoc-Cl (4.16 g, 16.12 mmol). The reaction was allowed to warm to room temperature overnight then acidified to pH 6 using dilute HCl. The reaction mixture was extracted with EtOAc (3 x 100 mL) and the combined organic layers were dried over anhydrous Na_2SO_4 and concentrated *in vacuo*. Purification by neutral silica gel column chromatography eluting with 40-100% EtOAc in *n*-hexane afforded ACC **2** as a white solid (1.5 g, 37% over 2 steps, 98% purity): mp 150.8-153.7 °C; ^{1}H NMR (400 MHz, DMSO-d_6) δ 12.34 (s, 1H), 7.89 (d, *J* = 7.6 Hz, 2H), 7.78 (s, 1H), 7.71 (m, 2H), 7.41 (m, 2H), 7.32 (m, 2H), 5.81 (m, 1H), 5.03-4.94 (m, 2H), 4.33-4.24 (m, 3H), 2.14 (m, 2H), 1.61 (m, 2H), 1.37 (m, 1H), 1.10 (m, 1H), 0.74 (m, 1H); ^{13}C NMR (75 MHz, DMSO-d_6) δ 174.8, 157.2, 144.3, 144.2, 141.2, 139.0, 128.1, 127.5, 125.7, 120.6, 115.4, 65.8, 47.2, 37.9, 33.2, 27.7, 27.0, 22.1; HRMS (ESI) m/z: $[M - H]^-$ Calcd for $C_{23}H_{22}NO_4$ 376.1548; found 376.1549.

(1*R*,2*S*)-1-((((9*H*-Fluoren-9-yl)methoxy)carbonyl)amino)-2-(hept-6-en-1-yl)cyclopropane-1-carboxylic acid (1). To a stirred solution of (*R*)-**8** (4 g, 18.43 mmol) in CH_2Cl_2 (40 mL) at 0 °C was added K_2CO_3 (7.63 g, 55.29 mmol) followed by tetrabutylammonium bromide (5.94 g, 18.43 mmol) and stirred for 15 min. To this solution, **18**[80] (3.48 g, 27.64 mmol) was added dropwise at 0 °C and the resulting reaction mixture was stirred at room temperature for 2 h. The reaction mixture was filtered through a pad of Celite® and the filtrate was concentrated *in vacuo*. Purification by flash column chromatography eluting with 0-10% EtOAc in *n*-hexane afforded compound **19** as a thick, colourless oil (3.5 g, 59%): ^{1}H NMR (400 MHz, $CDCl_3$) δ 7.85 (d, *J* = 6.8 Hz, 2H), 7.48-7.46 (m, 3H), 6.93 (t, *J* = 8.0 Hz, 1 H), 5.84-5.77 (m, 1H), 5.56 (s, 1H), 4.99 (d, *J* = 17.2 Hz, 1H), 4.93 (d, *J* = 10.0 Hz, 1 H), 2.68 (q, *J* = 7.2 Hz, 2H), 2.20 (m, 1H), 2.06-2.04 (m, 2H), 1.43 (m, 4H), 1.13 (d, *J* = 6.8 Hz, 3H), 0.80 (d, *J* = 7.2 Hz, 3H).

To a suspension of trimethyl sulfoxonium chloride (4.1 g, 32.03 mmol) and NaH (1.2 g, 32.03 mmol) at 0 °C was added dry THF (60 mL) and the resulting reaction mixture was refluxed at 100 °C for 16 h. The reaction mixture was cooled to room temperature and the suspended solution was added to a cooled solution of **19** (3.5 g, 10.76 mmol) in THF (20 mL) *via* cannula. The reaction mixture was stirred at 0 °C for 1 h then at room temperature for another hour. Progress of the reaction was monitored by TLC. After completion, the reaction mixture was concentrated *in vacuo* and purified by flash column chromatography eluting with 0-10% EtOAc in *n*-hexane to afford **20** (1.7 g, 46.5 %) as an off-white solid. ^{1}H NMR (400 MHz, $CDCl_3$) δ 7.64 (d, *J* = 6.0 Hz, 2H), 7.44-7.42 (m, 3H), 5.85-5.79 (m, 1H), 5.61 (s, 1H), 5.00 (d, *J* = 17.2 Hz, 1H), 4.95 (d, *J* = 9.6 Hz, 1H), 2.16-2.06 (m, 5H), 1.74-1.69 (m, 2H), 1.46-1.41 (m, 7H), 1.12 (d, *J* = 6.4 Hz, 3H), 0.87 (d, J = 6.4 Hz, 3H); LCMS (ESI) m/z: $[M + H]^+$ Calcd for $C_{22}H_{30}NO_2$ 340.23; Found 340.14.

Aqueous NaOH (1.07 g, 24.33 mmol in 25 mL water) was added to a solution of **20** (1.65 g, 4.86 mmol) in EtOH (25 mL). The reaction mixture was stirred at room temperature for 48 h before the solvent was removed *in vacuo*. The crude material was re-dissolved in a mixture of THF and water (1:1, 50 mL) and cooled to 0 °C before the addition of Fmoc-Cl (1.88 g, 7.29 mmol). The reaction was allowed to warm to room temperature overnight then acidified to pH6 using dilute HCl. The reaction mixture was extracted with EtOAc (3 x 50 mL) and the combined organic layers were dried over anhydrous Na_2SO_4 and concentrated *in vacuo*. Purification by flash column chromatography eluting with 30-100% EtOAc in *n*-hexane afforded ACC **1** as a white solid (0.6 g, 30% over 2 steps, 93% purity): mp 162.7-165.3 °C;

^{1}H NMR (400 MHz, DMSO-d_6) δ 12.29 (s, 1H), 7.88 (d, J = 6.8 Hz, 2H), 7.73-7.68 (m, 3H), 7.41 (m, 2H), 7.31 (m, 2H), 5.79-5.73 (m, 1H), 4.97 (d, J = 17.2, 1H), 4.91 (d, J = 10.4, 1H), 4.32-4.17 (m, 3H), 1.99 (m, 2H), 1.55-1.30 (m, 9 H), 1.00 (m, 1H), 0.72 (m, 1H); ^{13}C NMR (75 MHz, DMSO-d_6) δ 174.9, 157.1, 144.3, 144.2, 141.2, 139.3, 128.1, 127.5, 125.7, 120.6, 115.1, 65.8, 47.2, 37.9, 33.6, 28.9, 28.8, 28.7, 28.1, 27.4, 22.1; HRMS (ESI) m/z: $[M - H]^-$ Calc for $C_{26}H_{28}NO_4$ 418.2018; found 418.2032.

Stapled peptide preparation. Dry resin (0.1 mmol) was swelled with DMF for 20 min before use. The Fmoc-protected amino acids (5 equiv.) were coupled using pre-activated (7 min) solutions of HATU (4.9 equiv.) and DIPEA (5 equiv.) in NMP (0.5 M) for 60 min except for R8, S5, ACC's **1** and **2**, which were pre-activated and coupled (2 equiv.) for 90 min. The amino acids immediately following the α,α-disubstituted amino acids were double coupled. The Fmoc protecting group was removed by treatment with 20% piperidine in DMF for 15 min. Following deprotection of the final Fmoc group, the peptides were acetylated using a mixture of acetic anhydride:DIPEA:DMF (2:2:1) for 60 min. After each coupling, deprotection and acetylation reaction, the resin was thoroughly washed with NMP. Ring-closing metathesis was performed using a solution of Grubbs I catalyst (20 mol%, 5 mg mL^{-1}) in dry 1,2-dichloroethane (DCE) at room temperature. The reaction was agitated by bubbling with argon gas (3 x 2 h treatments, with the addition of fresh catalyst solution at the start of each cycle). The reaction mixture was drained, the resin washed with DMSO:DMF (1:1, 2 h), DCE (3 x 1 min) and MeOH (3 x 1 min) then dried under vacuum. Cleavage of the peptide from the resin was achieved using a TFA cocktail consisting TFA-triisopropylsilane:water (95:2.5:2.5, 8 mL) for 2 h followed by filtration and precipitation with diethyl ether. The precipitate was collected by centrifugation.

Fluorescence Anisotropy Competition Assay: Fluorescence anisotropy assays were performed as previously described.[23] Titrations of purified MDM2/MDM4 proteins were incubated with 50 nM of carboxyfluorescein (FAM) labelled 12-1 peptide (FAM-RFMDYWEGL-NH_2) to initially determine the dissociation constants for the peptide-protein interaction. Apparent K_ds of peptides were next determined by competitive fluorescence anisotropy. Titrations of peptides were carried out at constant concentrations of MDM2/MDM2-M62A/MDMX (150 nM), MDMX-L98V (250 nM) and labelled peptide (50 nM). Anisotropy measurements were carried out using the Envision Multilabel Reader (PerkinElmer). All experiments were carried out in PBS (2.7 mM KCl, 137 mM NaCl, 10 mM Na_2HPO_4 and 2 mM KH_2PO_4, pH 7.4), 3% DMSO v/v and 0.1% Tween-20 v/v buffer. All titrations were carried out in duplicate. Curve fitting was carried out using Prism 5.0 (GraphPad).

T22 p53 reporter assay: T22 p53 β-galactosidase based reporter assay T22 cells, which were stably transfected with a p53 responsive β-galactosidase reporter, were seeded into 96-well plate at a cell density of 8000 cells per well.[93] Cells were also maintained in Dulbecco's Minimal Eagle Medium (DMEM) with 10% fetal calf serum (FCS) and penicillin/streptomycin. The cells were incubated for 24 hours and then the media was removed and replaced with 90 µl of DMEM either with 0% or 10% FCS. Cells were treated with compounds/peptide for 18 hours in DMEM with 0% or 10% FCS. Final working concentration of DMSO after compound addition was 1% v/v. Corresponding negative control wells with 1% DMSO only were also prepared. β-galactosidase activity was detected using the FluoReporter LacZ/Galactosidase Quantitation kit (Invitrogen) as per manufacturer's instructions. Measurements were carried out using an Envision multiplate reader (Perkin-Elmer). Experiments were carried out independently twice.

Molecular dynamics: Chains A and C from the crystal structure of M06 peptide complexed with the N-terminal domain of MDM2-M62A (PDB code 4UMN[94]) were used as the initial structures for molecular dynamics (MD) simulations. M06 was converted to sMTide-02 by mutating Trp23 to Ala. MDM2 was converted to its wild type state by reversing the M62A mutation, and its N-terminal residues 18-24 deleted to facilitate convergence of binding free energy calculations. Residue protonation states were determined by PDB2PQR.[95] The LEaP program in the AMBER 18[96] package was then used to solvate each system with TIP3P[97] water molecules in a periodic truncated octahedron box, such that its walls were at least 10 Å away from the MDM2-peptide complex and 15 Å away from the free peptide, and for neutralization of charges with chloride ions.

Energy minimizations and MD simulations were performed with the PMEMD module of AMBER 18.[96] Four independent explicit-solvent MD simulations using different initial atomic velocities were carried out on each of the free peptides, sMTide-02, VIP141, VIP142 and dicyclopropane-substituted sMTide-02, and their complexes with MDM2 using the ff14SB[98] and generalized AMBER force fields (GAFF).[99] Atomic charges for the stapled residues were derived using the R.E.D. Server,[100] which fits restrained electrostatic potential (RESP) charges[101] to a molecular electrostatic potential (MEP) computed by the Gaussian 09 programme[102] at the HF/6-31G* theory level. All bonds involving hydrogen atoms were constrained by the SHAKE algorithm[103], allowing for a time step of 2 fs. Nonbonded interactions were truncated at 9 Å while electrostatic interactions were treated by the particle mesh Ewald method.[104] Energy minimisation was carried out using the steepest descent algorithm for 500 steps, followed by the conjugate gradient algorithm for another 500 steps. The system was then heated gradually to 300 K over 50 ps at constant volume before equilibration at a constant pressure of 1 atm for another 50 ps. Weak harmonic positional restraints with a force constant of 2.0 kcal mol^{-1} $Å^{-2}$ were imposed on the non-hydrogen atoms of the solute during minimisation and equilibration. Subsequent unrestrained equilibration (2 ns) and production (200 ns) runs were carried out at 300 K and 1 atm. The temperature was maintained using a Langevin thermostat[105] with a collision frequency of 2 ps^{-1} while the pressure was maintained by a Berendsen barostat[106] with a pressure relaxation time of 2 ps.

Binding free energy calculations: Binding free energies for the MDM2 complexes were calculated using the molecular mechanics/generalized Born surface area (MM/GBSA) method[107] implemented in AMBER 18. Two hundred equally-spaced snapshot structures were extracted from the last 60-80 ns or each of the trajectories, and their molecular mechanical energies calculated with the sander module. The polar contribution to the solvation free energy was computed by the pbsa[108] program using the modified generalised Born model described by Onufriev *et al.*[109] while the nonpolar contribution was estimated from the solvent accessible surface area using the molsurf[110] program with $\gamma = 0.005$ kcal $Å^{-2}$ and β set to zero. Entropy change for the peptides was assumed to be similar and therefore omitted from the calculations.

Conformational clustering: Backbone atoms of peptide residues were clustered using the MMTSB toolset.[111] The ART-2 algorithm[112, 113] was used for root-mean-square-deviation-based clustering. Cutoff radii of 3.7 Å, 3.2 Å,3.6 Å and 3.3 Å were empirically chosen to produce well-separated clusters for sMTide-02, VIP141, VIP142, and dicyclopropane-substituted sMTide-02 respectively.

Supporting Information

- Characterisation data for compounds **1**, **2**, **13**, **14**, **19** and **20**
- HPLC chromatograms of **VIP141-145**

Author Information

Corresponding Author. *E-mail: yuenty@ices.a-star.edu.sg
ORCID. Tsz Ying Yuen: 0000-0001-7971-1726
Charles W. Johannes: 0000-0002-5170-058X
Author Contributions. T.Y.Y., C.J.B., Y. S. T. and C.W.J. contributed equally.
Notes. The authors declare no competing financial interest.

Acknowledgements

This research was funded by the A*STAR JCO Visiting Investigatorship Programme (JCO 1235d00048) and the Industry Alignment Fund (Pre-position, HBMS domain H17/01/a0/010). We thank Prof. Greg Verdine for his scientific input as the visiting investigator. We also thank Sai Life Sciences Limited for synthesis support.

References

1. Wells, J. A. McClendon, C. L., Reaching for high-hanging fruit in drug discovery at protein-protein interfaces. *Nature* **2007,** *450*, 1001.
2. Ivanov, A. A. Khuri, F. R.; Fu, H., Targeting protein-protein interactions as an anticancer strategy. *Trends Pharmacol. Sci.* **2013,** *34*, 393.
3. Garner, A. L. Janda, K. D., Protein-protein interactions and cancer: targeting the central dogma. *Curr. Top. Med. Chem.* **2011,** *11*, 258.
4. Brown, C. J. Lian, S.; Verma, C. S.; Fersht, A. R.; Lane, D. P., Awakening guardian angels: drugging the p53 pathway. *Nat. Rev. Cancer* **2009,** *9*, 862.
5. Chene, P., Inhibiting the p53-MDM2 interaction: an important target for cancer therapy. *Nat. Rev. Cancer* **2003,** *3*, 102.
6. Chene, P., Inhibition of the p53-MDM2 interaction: targeting a protein-protein interface. *Mol. Cancer Res.* **2004,** *2*, 20.
7. Iwakuma, T. Lozano, G., MDM2, an introduction. *Mol. Cancer Res.* **2003,** *1*, 993.
8. Nag, S. Zhang, X.; Srivenugopal, K. S.; Wang, M.-H.; Wang, W.; Zhang, R., Targeting MDM2-p53 interaction for cancer therapy: are we there yet? *Curr. Med. Chem.* **2014,** *21*, 553.
9. Nag, S. Qin, J.; Srivenugopal, K. S.; Wang, M.; Zhang, R., The MDM2-p53 pathway revisited. *J. Biomed. Res.* **2013,** *27*, 254.
10. Arkin, M. R. Tang, Y.; Wells, J. A., Small-molecule inhibitors of protein-protein interactions: progressing toward the reality. *Chem. Biol.* **2014,** *21*, 1102.
11. Smith, M. C. Gestwicki, J. E., Features of protein-protein interactions that translate into potent inhibitors: topology, surface area and affinity. *Expert Rev. Mol. Med.* **2012,** *26*, e16.
12. Scott, D. E. Bayly, A. R.; Abell, C.; Skidmore, J., Small molecules, big targets: drug discovery faces the protein-protein interaction challenge. *Nat. Rev. Drug Discov.* **2016,** *15*, 533.
13. Cukuroglu, E. Engin, H. B.; Gursoy, A.; Keskin, O., Hot spots in protein-protein interfaces: towards drug discovery. *Prog. Biophys. Mol. Biol.* **2014,** *116*, 165.
14. Jochim, A. L. Arora, P. S., Systematic analysis of helical protein interfaces reveals targets for synthetic inhibitors. *ACS Chem. Biol.* **2010,** *5*, 919.
15. Raj, M. Bullock, B. N.; Arora, P. S., Plucking the high hanging fruit: a systematic approach for targeting protein-protein interactions. *Bioorg. Med. Chem.* **2013,** *21*, 4051.
16. Grigoryev, Y., Stapled peptide to enter human testing, but affinity questions remain. *Nat. Med.* **2013,** *19*, 120.
17. Payton, M. Pinchasik, D.; Mehta, A.; Goel, S.; Zain, J. M.; Sokol, L.; Jacobsen, E.; Patel, M. R.; Horwitz, S. M.; Meric-Bernstam, F; Shustov, A.; Weinstock, D.; Avivado, M.; Annis, D. A., Phase 2a study

of a novel stapled peptide ALRN-6924 disrupting MDMX- and MDM2-mediated inhibition of wild-type TP53 in patients with peripheral t-cell lymphoma. *Ann. Oncol.* **2017,** *28*, 355.

18. Meric-Bernstam, F. Saleh, M. N.; Infante, J. R.; Goel, S.; Falchook, G. S.; Shapiro, G., Phase I trial of a novel stapled peptide ALRN-6924 disrupting MDMX- and MDM2-mediated inhibition of WT p53 in patients with solid tumors and lymphomas. *J. Clin. Oncol.* **2017,** *26*, 153.

19. Miller, S. J. Grubbs, R. H., Synthesis of conformationally restricted amino acids and peptides employing olefin metathesis. *J. Am. Chem. soc.* **1995,** *117*, 5855.

20. Blackwell, H. E. Sadowsky, J. D.; Howard, R. J.; Sampson, J. N.; Chao, J. A.; Steinmetz, W. E.; O'Leary, D. J.; Grubbs, R. H., Ring-closing metathesis of olefinic peptides: design, synthesis, and structural characterization of macrocyclic helical peptides. *J. Org. Chem.* **2001,** *66*, 5291.

21. Blackwell, H. E. Grubbs, R. H., Highly efficient synthesis of covalently cross-linked peptide helices by ring-closing metathesis. *Angew. Chem. Int. Ed.* **1998,** *37*, 3281.

22. Schafmeister, C. E. Po, J.; Verdine, G. L., An all-hydrocarbon cross-linking system for enhancing the helicity and metabolic stability of peptides. *J. Am. Chem. Soc.* **2000,** *122*, 5891.

23. Brown, C. J. Quah, S. T.; Jong, J.; Goh, A. M.; Chiam, P. C.; Khoo, K. H.; Choong, M. L.; Lee, M. A.; Yurlova, L.; Zolghadr, J.; Joseph, T. L.; Verma, C. S.; Lane, D. P., Stapled peptides with improved potency and specificity that activate p53. *ACS Chem. Biol.* **2013,** *8*, 506.

24. Chang, Y. S. Graves, B.; Guerlavais, V.; Tovar, C.; Packman, K.; To, K.-H.; Olson, K. A.; Kesavan, K.; Gangurde, P.; Mukherjee, A.; Baker, T.; Darlak, K.; Elkin, C.; Filipovic, Z.; Qureshi, F. Z.; Cai, H.; Berry, P.; Feyfant, E.; Shi. X, E.; Horstick, J.; Annis, D. A.; Manning, A. M.; Fotouhi, N.; Nash, H.; Vassilev, L. T.; Sawyer, T. K., Stapled α-helical peptide drug development: a potent dual inhibitor of MDM2 and MDMX for p53-dependent cancer therapy. *Proc. Natl. Acad. Sci. USA.* **2013,** *110*, E3445.

25. Walensky, L. D. Kung, A. L.; Escher, I.; Malia, T. J.; Barbuto, S.; Wright, R. D.; Wagner, G.; Verdine, G. L.; Korsmeyer, S. J., Activation of apoptosis in vivo by a hydrocarbon-stapled BH3 helix. *Science* **2004,** *305*, 1466.

26. Danial, N. N. Walensky, L. D.; Zhang, C. Y.; Choi, C. S.; Fisher, J. K.; Molina, A. J.; Datta, S. R.; Pitter, K. L.; Bird, G. H.; Wikstrom, J. D.; Deeney, J. T.; Robertson, K.; Morash, J.; Kulkarni, A.; Neschen, S.; Kim, S.; Greenberg, M. E.; Corkey, B. E.; Shirihai, O. S.; Shulman, G. I.; Lowell, B. B.; Korsmeyer, S. J., Dual role or proapoptotic BAD in insulin secretion and beta cell survival. *Nat. Med.* **2008,** *14*, 144.

27. Grossman, T. N. Yeh, J. T.; Bowman, B. R.; Chu, Q.; Moellering, R. E.; Verdine, G. L., Inhibition of oncogenic Wnt signaling through direct targeting of β-catenin. *Proc. Natl. Acad. Sci. USA.* **2012,** *109*, 17942.

28. Lama, D. Liberatore, A.-M.; Frosi, Y.; Nakhle, J.; Tsomaia, N.; Bashir, T.; Lane, D. P.; Brown, C. J.; Verma, C. S.; Auvin, S., Structural insights reveal a recognition feature for tailoring hydrocarbon stapled-peptides against the eukaryotic translation initiation factor 4E protein. *Chem. Sci.* **2019,** *10*, 2489.

29. Bird, G. H. Madani, N.; Perry, A. F.; Princiotto, A. M.; Supko, J. G.; He, X.; Gavathiotis, E.; Sodroski, J. G.; Walensky, L. D., Hydrocarbon double-stapling remedies the proteolytic instability of a lengthy peptide therapeutic. *Proc. Natl. Acad. Sci. USA.* **2010,** *107*, 14093.

30. Gaillard, V. Galloux, M.; Garcin, D.; Eléouët, J.-F.; Goffic, R. L.; Larcher, T.; Rameix-Welti, M.-A.; Boukadiri, A.; Héritier, J.; Segura, J.-M.; Baechler, E.; Arrell, M.; Mottet-Osman, G.; Nyanguile, O., A short double-stapled peptide inhibits respiratory syncytial virus entry and spreading. *Antimicrob. Agents Chemother.* **2017,** *61*, E02241-16.

31. Cromm, P. M. Spiegel, J.; Küchler, P.; Dietrich, L.; Kriegesmann, J.; Wendt, M.; Goody, R. S.; Waldmann, H.; Grossmann, T. N., Protease-resistant and cell-permeble double-stapled peptides targeting the Rab8a GTPase. *ACS Chem. Biol.* **2016,** *11*, 2375.

32. Cromm, P. M. Schaubch, S.; Spiegel, J.; Fürstner, A.; Grossmann, T. N.; Waldmann, H., Orthogonal ring-closing alkyne and olefin metathesis for the synthesis of small GPTase-targeting bicyclic peptides. *Nat. Commun.* **2016,** *7*, 1.

33. Hilinski, G. J. Kim, Y. W.; Hong, J.; Kutchukian, P. S.; Crenshaw, C. M.; Berkovitch, S. S.; Chang, A.; Ham, S.; Verdine, G. L., Stitched α-helical peptides via bis ring-closing metathesis. *J. Am. Chem. Soc.* **2014,** *136*, 12314.
34. Toniolo, C. Benedetti, E., Structures of polypeptides from α-amino acids disubstituted at the α-carbon. *Macromolecules* **1991,** *24*, 4004.
35. Demizu, Y. Doi, M.; Kurihara, M.; Okuda, H.; Nagano, M.; Suemune, H.; Tanaka, M., Conformational studies on peptides containing α,α-disubstituted α-amino acids: chiral cyclic α,α-disubstituted α-amino acids as an α-helical inducer. *Org. Biol. Chem.* **2011,** *9*, 3303.
36. Toniolo, C. Crisma, M.; Formaggio, F.; Peggion, C., Control of peptide conformation by the Thorpe-Ingold effect (C alpha-tetrasubstitution). *Biopolymers* **2001,** *60*, 396.
37. Boal, A. K. Guryanov, I.; Moretto, A.; Crisma, M.; Lanni, E. L.; Toniolo, C.; Grubbs, R. H.; O'Leary, D. J., Facile and E-selective intramolecular ring-closing metathesis reactions in 310-helical peptides: a 3D structural study. *J. Am. Chem. Soc.* **2007,** *129*, 6986.
38. Bernal, F. Tyloer, A. F.; Korsmeyer, S. J.; Walensky, L. D.; Verdine, G. L., Reactivation of the p53 tumor suppressor pathway by a stapled p53 peptide. *J. Am. Chem. Soc.* **2007,** *129*, 2456.
39. Moellering, R. E. Cormejo, M.; Davis, T. N.; Del Bianco, C.; Aster, J. C.; Blacklow, S. C.; Kung, A. L.; Gilliland, D. G.; Verdine, G. J.; Bradner, J. E., Direct inhibition of the NOTCH transcription factor complex. *Nature* **2009,** *462*, 182.
40. Zhang, F. Sadovski, O.; Xin, S. J.; Woolley, G. A., Stabilization of folded peptide and protein structures via distance matching with a long, rigid cross-linker. *J. Am. Chem. Soc.* **2007,** *129*, 14154.
41. Toledo-Sherman, L. M. Prime, M. E.; Mrzljak, L.; Beconi, M. G.; Beresford, A.; Brookfield, F. A.; Brown, C. J.; Cardaun, I.; Courtney, S. M.; Dijkman, U.; Hamelin-Flegg, E.; Johnson, P. D.; Kempf, V.; Lyons, K.; Matthews, K.; Mitchell, W. L.; O'Connell, C.; Pena, P.; Powell, K.; Rassoulpour, A.; Reed, L.; Reindl, W.; Selvaratnam, S.; Friley, W. W.; Weddell, D. A.; Went, N. E.; Wheelan, P.; Winkler, C.; Winkler, D.; Wityak, J.; Yarnold, C. J.; Yates, D.; Munoz-Sanjuan, I.; Dominguez, C., Development of a series of aryl pyrimidine kynurenine monooxygenase inhibitors as potential therapeutic agents for the treatment of Huntington's disease. *J. Med. Chem.* **2015,** *58*, 1159.
42. Jin, C. Decker, A. M.; Harris, D. L.; Blough, B. E., Effect of substitution on the aniline moiety of the GRP88 agonist 2-PCCA: synthesis, structure-activity relationships, and molecular modeling studies. *ACS Chem. Neurosci.* **2016,** *7*, 1418.
43. Taber, M. T. Wright, R. N.; Molski, T. F.; Clarke, W. J.; Brassil, P. J.; Denhart, D. J.; Mattson, R. J.; Lodge, N. J., Neurochemical, pharmacokinetic, and behavioral effects of the novel selective serotonin reuptake inhibitor BMS-505130. *Pharmacol. Biochem. Behav.* **2005,** *80*, 521.
44. Tedford, C. E. Phillips, J. G.; Gregory, R.; Pawlowski, G. P.; Fadnis, L.; Khan, M. A.; Ali, S. M.; Handley, M. K.; Yates, S. L., Development of trans-2-[1H-imidazol-4-yl] cyclopropane derivatives as new high-affinity histamine H3 receptor ligands. *J. Pharmacol. Exp. Ther.* **1999,** *289*, 1160.
45. Burroughs, L., I-aminocyclopropane-I-carboxylic acid: a new amino-acid in perry pears and cider apples. *Nature* **1957,** *179*, 360.
46. Virtanen, A. I. Vahatalo, M. L., A new cyclic α-aminocarboxylic acid in berries of cowberry. *Acta Chem. Scand.* **1957,** *11*, 741.
47. Ichihara, A. Shiraishi, K.; Sato, H.; Sakamura, S.; Nishiyama, K.; Sakai, R.; Furusaki, A.; Matsumoto, T., The structure of coronatine. *J. Am. Chem. Soc.* **1977,** *99*, 636.
48. Mitchell, R. E., Norcoronatine and N-coronafacoyl-L-valine, phytotoxic analogues of coronatine produced by a strain of Pseudomonas syringae pv. glycinea. *Phytochemistry* **1985,** *24*, 1485.
49. Wakamiya, T. Nakamoto, H.; Shiba, T., Structural determination of carnosadine, a new cyclopropyl amino acid, from red alga Grateloupia carnosa. *Tetrahedron Lett.* **1984,** *25*, 4411.
50. Mizuno, A. Matsui, K.; Shuto, S., The use of cyclopropane in peptidomimetic chemistry. *Chem. Eur. J.* **2017,** *23*, 14394.

51. Vaughn, L. K. Wire, W. S.; Davis, P.; Shimohigashi, Y.; Toth, G.; Knapp, R. J.; Hruby, V. J.; Burks, T. F.; Yamamura, H. I., Differentiation between rat brain and mouse vas deferens δ opioid receptors. *Eur. J. Pharmacol.* **1990,** *177*, 99.
52. Moye-Sherman, D. Jin, S.; Li, S.; Welch, M. B.; Reibenspies, J.; Burgess, K., Cyclopropane amino acids that mimic two χ1-conformations of phenylalanine. *Chem. Eur. J.* **1999,** *5*, 2730.
53. Moye-Sherman, D. Jin, S.; Ham, I.; Lim, D.; Scholtz, M.; Burgess, K., Conformational preferences of RNase A C-peptide derivatives containing a highly constrained analogue of phenylalanine. *J. Am. Chem. Soc.* **1998,** *120*, 9435.
54. Burgess, K. L.i W., Syntheses of Fmoc-2,3-methanoleucine stereoisomers and their incorporation into peptidomimetics. *Methods Mol. Med.* **1999,** *23*, 25.
55. Rancourt, J. Cameron, D. R.; Gorys, V.; Lamarre, D.; Poirier, M.; Thibeault, D.; Llinàs-Brunet, Peptide-based inhibitors of the Hepatitis C virus NS3 protease: structure-activity relationship at the C-terminal position. *J. Med. Chem.* **2004,** *47*, 2511.
56. Goudreau, N. Brochu, C.; Cameron, d. R.; Duceppe, J.-S.; Faucher, A.-M.; Ferland, J.-M.; Grand-Maître; Poirier, M.; Simoneau, B.; Tsantrizos, Y. S., Potent inhibitors of the hepatitis C virus NS3 protease: design and synthesis of macrocyclic substrate-based β-strand mimics. *J. Org. Chem.* **2004,** *69*, 6185.
57. Tsantrizos, Y. S. Ferland, J.-M.; McClory, A.; Poirier, M.; Farina, V.; Yee, N. K.; Wang, X.-J.; Haddad, N.; Wei, X.; Xu, J.; Zhang, L., Olefin ring-closing metathesis as a powerful tool in drug discovery and development - potent macrocyclic inhibitors of the hepatitis C virus NS3 protease. *J. Organomet. Chem.* **2006,** *691*, 5163.
58. Beaulieu, P. L. Gillard, J.; Bailey, M. D.; Boucher, C.; Duceppe, J.-S.; Simoneau, B.; Wang, X.-J.; Zhang, L.; Grozinger, K.; Houpis, I.; Farina, V.; Heimroth, H.; Krueger, T.; Schnaubelt, J., Synthesis of (1R,2S)-1-amino-2-vinylcyclopropanecarboxylic acid vinyl-ACCA) derivatives: key intermediates for the preparation of inhibitors of the Hepatitis C Virus NS3 protease. *J. Org. Chem.* **2005,** *70*, 5869.
59. Chaplin, D. A. Fox, M. E.; Kroll, S. H. B., Dynamic kinetic resolution of dehydrocoronamic acid. *Chem. Commun.* **2014,** *50*, 5858.
60. Tang, W. Wei, X.; Yee, N. K.; Patel, N.; Lee, H.; Savoie, J.; Senanayake, C. H., A practical asymmetric synthesis of isopropyl (1R,2S)-dehydrocoronamate. *Org. Process Res. Dev.* **2011,** *15*, 1207.
61. Kawashima, A. Xie, C.; Mei, H.; Takeda, R.; Kawamura, A.; Sato, T.; Moriwaki, H.; Izawa, K.; Han, J.; Aceña, J. L.; Soloshonok, V. A., Asymmetric synthesis of (1R,2S)-1-amino-2-vinylcyclopropanecarboxylic acid by sequential SN2-SN2' dialkylation of (R)-N-(benzyl)proline-derived glycine Schiff base Ni(II) complex. *RSC Adv.* **2015,** *5*, 1051.
62. Kawashima, A. Shu, S.; Takeda, R.; Kawamura, A.; Sato, T.; Moriwaki, H.; Wang, J.; Izawa, K.; Aceña, J. L.; Soloshonok, V. A. Liu, H., Advanced asymmetric synthesis of (1R,2S)-1-amino-2-vinylcyclopropanecarboxylic acid by alkylation/cyclization of newly designed axially chiral Ni(II) compex of glycine Schiff base. *Amino Acids* **2016,** *48*, 973.
63. Belyk, K. M. Xiang, B.; Bulger, P. G.; Leonard, Jr., W. R.; Balsells, J.; Yin, J.; Chen, C., Enantioselective synthesis of (1R,2S)-1-amino-2-vinylcyclopropanecarboxylic acid ethyl ester (vinyl-ACCA-OEt) by asymmetric phase-transfer catalyzed cyclopropanation of (E)-N-phenylmethyleneglycine ethyl ester. *Org. Process Res. Dev.* **2010,** *14*, 692.
64. Fox, M. E. Lennon, I. C.; Farina, V., Catalytic asymmetric synthesis of ethyl (1R,2S)-dehydrocoronamate. *Tetrahedron Lett.* **2007,** *48*, 945.
65. Adams, L. A. Aggarwal, V. K.; Bonnert, R. V.; Bressel, B.; Cox, R. J.; Shepherd, J.; de Vicente, J.; Walter, M.; Whittingham, W. G.; Winn, C. L., Diastereoselective synthesis of cyclopropane amino acids using diazo compounds generated in situ. *J. Org. Chem.* **2003,** *68*, 9433.
66. Koskinen, A. M. P. Muñoz, L., Intramolecular cyclopropanation: stereospecific synthesis of (E)- and (Z)-1-aminocyclopropane-1-carboxylic acids. *J. Org. Chem.* **1993,** *58*, 879.
67. Lindsay, V. N. G. Lin, W.; Charette, A. B., Experimental evidence for the all-up reactive conformation of chiral rhodium(II) carboxylate catalysts: enantioselective synthesis of cis-cyclopropane α-amino acids. *J. Am. Chem. Soc.* **2009,** *131*, 16383.

68. Moreau, B. Charette, A., Expedient synthesis of cyclopropane α-amino acids by the catalytic asymmetric cyclopropanation of alkenes using iodonium ylides derived from methyl nitroacetate. *J. Am. Chem. Soc.* **2005,** *127*, 18014.
69. Moreau, B. Alberico, D.; Lindsay, N. G.; Charette, Enantioselective one-pot three-component synthesis of propargylamines catalyzed by copper(I)-pyridine bis-(oxazoline) complexes. *Tetrahedron* **2012,** *68*, 3487.
70. Chinchilla, R. Falvello, L. R.; Galindo, N.; Nájera, C., New chiral didehydroamino acid derivatives from a cyclic glycine template with 3,6-dihydro-2H-1,4-oxazin-2-one structure: applications to the asymmetric synthesis of nonproteinogenic α-amino acids. *J. Org. Chem.* **2000,** *65*, 3034.
71. Abellán, T. Chinchilla, R.; Galindo, N.; Nájera, C.; Sansano, J. M., New oxazinone and pyrazinone derivatives as chiral reagents for the asymmetric synthesis of α-amino acids. *J. Heterocyclic Chem.* **2000,** *37*, 467.
72. Horner, L. Hoffmann, H.; Wippel, H. G., Phosphororganische verbindungen, XII. phosphinoxyde als olefinierungsreagenzien. *Chem. Ber.* **1958,** *91*, 61.
73. Horner, L. Hoffman, H.; Wippel, H. G.; Klahre, G., Phosphororganische verbindungen, XX. phosphinoxyde als olefinierungsreagenzien. *Chem. Ber.* **1959,** *92*, 2499.
74. Wadsworth, W. S.; Jr., Emmons, W. D., The utility of phosphonate carbanions in olefin synthesis. *J. Am. Chem. Soc.* **1961,** *83*, 1733.
75. Wadsworth, D. H. Schupp, I. O. E.; Sous, E. J.; Ford, J. J. A., The stereochemistry of the phosphonate modification of the Wittig reaction. *J. Org. Chem.* **1965,** *30*, 680.
76. Alami, A. Calmes, M.; Daunis, J.; Escale, F.; Jacquier, R.; Roumestant, M.-L.; Viallefont, P., Asymmetric synthesis of cis and trans 2-methyl and 2-ethyl 1-amino cyclopropanecarboxylic acids. *Tetrahedron: Asymmetry* **1991,** *2*, 175.
77. Cativiela, C. Diaz-de-Villegas, M. D.; Gálvez, J. A., Efficient asymmetric synthesis of amino acids through hydrogenation of the didehydroamino acid residue in cyclic imino-ester derivatives. *Tetrahedron: Asymmetry* **1992,** *3*, 567.
78. Calmes, M. Daunis, J.; Escale, F., Synthesis of enantiomerically pure 2-alkyl 1-amino cyclopropane-1-carboxylic acid. *Tetrahedron: Asymmetry* **1996,** *7*, 395.
79. Corey, E. J. Chaykovsky, J., Dimethyloxosulfonium methylide ((CH3)2SOCH2) and dimethylsulfonium methylide ((CH3)2SCH2). Formation and application to organic synthesis. *J. Am. Chem. Soc.* **1965,** *87*, 1353.
80. Halle, M. B. Fernandes, R. A., A relay ring-opening/double ring-closing metathesis strategy for the bicyclic macrolide-butenolide core structures. *RSC Adv.* **2014,** *4*, 63342.
81. Thean, D. Ebo, J. S.; Luxton, T.; Lee, X. C.; Yuen, T. Y.; Ferrer, F. J.; Johannes, C. W.; Lane, D. P.; Brown, C. J., Enhancing specific disruption of intracellular protein complexes by hydrocaron stapled peptides using lipid based delivery. *Sci. Rep.* **2017,** *7*, 1763.
82. Yuen, T. Y. Brown, C. J.; Xue, Y. Z.; Tan, Y. S.; Ferrer Gago, F. J.; Lee, X. E.; Neo, J. Y.; Thean, D.; Kaan, H. Y. K.; Partridge, A. W.; Verma, C. S.; Lane, D. P.; Johannes, C. W., Stereoisomerism of stapled peptide inhibitors of the p53-Mdm2 interaction: an assessment of synthetic strategies and activity profiles. *Chem. Sci.* **2019,** *10*, 6457.
83. Zhang, R. Mayhood, T.; Lipari, P.; Wang, Y.; Durkin, J.; Syto, R.; Gesell, J.; McNemar, C.; Windsor, W., Fluorescence polarization assay and inhibitor design for MDM2/p53 interaction. *Anal. Biochem.* **2004,** *331*, 138.
84. Walensky, L. D. Bird, G. H., Hydrocarbon-stapled peptides: principles, practice, and progress. *J. Med. Chem.* **2014,** *57*, 6275.
85. Bottger, A. Bottger, V.; sparks, A.; Liu, W. L.; Howard, S. F.; Lane, D. P., Design of a synthesis Mdm2-binding mini protein that activates the p53 resposne in vivo. *Curr. Biol.* **1997**, 7.
86. Dastidar, S. G. Lane, D. P.; Verma, C. S., Why is F19Asp53 unable to bind MDM2? Simulatiosn suggest crack propagation modulates binding. *Cell Cycle* **2012,** *11*, 2239.

87. Sun, S. Zhao, G.; Huang, Y.; Cai, M.; Yan, Q.; Wang, H.; Chen. Y., Enantiomeric effect of D-amino acid substitution on the mechanism of action of α-helical membrane-active peptides. *Int. J. Mol. Sci.* **2018,** *19*, 67.
88. Huang, Y. He, L.; Li, G.; Zhai, N.; Jiang, H.; Chen. Y., Role of helicity of α-helical antimicrobial peptides to improve specificity. *Protein Cell* **2014,** *5*, 631.
89. Chen, Y. Mant, C. T.; Farmer, S. W.; Hancock, R. E. W.; Vasil, M. L.; Hodges, R. S., Rational design of α-helical antimicrobial peptides with enhanced activities and specificity/therapeutic index. *J. Biol. Chem.* **2005,** *280*, 12316.
90. Bird, G. H. Mazzola, E.; Opoku-Nsiah, K.; Lammert, M. A.; Godes, M.; Neuberg, D. S.; Walensky, L. D., Biophysical determinants for cellular uptake of hydrocarbon-stapled peptide helices. *Nat. Chem. Biol.* **2016,** *12*, 845.
91. Partridge, A. W. Kaan, H. Y. K.; Juang, Y.-C.; Sadruddin, A.; Lim, S.; Brown, C. J.; Ng, S.; Thean, D.; Ferrer, F.; Johannes, C.; Yuen, T. Y.; Kannan, S.; Aronica, P.; Tan, Y. S.; Pradhan, M. R.; Verma, C. S.; Hochman, J.; Chen, S.; Wan, H.; Ha, S.; Sherborne, B.; Lane, D. P.; Sawyer, T. K., Incorporation of putative helix-breaking amino acids in the design of novel stapled peptides: exploring biophysical and cellular permeability properties. *Molecules* **2019,** *24*, 2292.
92. Sakagami, K. Masuda, T.; Kawano, K.; Futaki, S., Importance of net hydrophobicity in the cellular uptake of all-hydrocarbon stapled peptides. *Mol. Pharmaceutics* **2018,** *15*, 1332.
93. Lu, X. Burbridge, S. A.; Griffin, S.; Smith, H. M., Discordance between accumulated p53 protein level and its transcriptional activity in response to u.v. radiation. *Oncogene* **1996,** *13*, 413.
94. Chee, S. M. Q. Wongsantichon, J.; Tng, Q. S.; Robinson, R.; Joseph, T. L.; Verma, C.; Lane, D. P.; Brown, C. J.; Ghadessy, F. J., Structure of a stapled peptide antagonist bound to nutlin-resistant Mdm2. *PLoS One* **2014**, 9.
95. Dolinsky, T. J. Nielsen, J. E.; McCammon, J. A.; Baker, N. A., PDB2PQR: an automated pipeline for the setup of Poisson-Boltzmann electrostatics calculations. *Nucleic Acids Res.* **2004,** *32*, W665.
96. Case, D. A. Ben-Shalom, I. Y.; Brozell, S. R.; Cerutti, D. S.; Cheatham, T. E., III; Cruzeiro, V. W. D.; Darden, T. A.; Duke, R. E.; Ghoreishi, D.; Gilson, M. K.; Gohlke, H.; Goetz, A. W.; Greene, D.; Harris, R.; Homeyer, N.; Izadi, S.; Kovalenko, A.; Kurtzman, T.; Lee, T. S.; LeGrand, S.; Li, P.; Lin, C.; Liu, J.; Luchko, T.; Leuo, R.; Mermelstein, D. J.; Merz, K. M.; Miao, Y.; Monard, G.; Nguygen, C.; Nguygen, H.; Omelyan, I.; Onufriev, A.; Pan, F.; Qi, R.; Roe, D. R.; Roitberg, A.; Sagui, C.; Schott-Verdugo, S.; Shen, J.; Simmerling, C. L.; Smith, J.; Salomon-Ferrer, R.; Swails, J.; Walker, R. C.; Wang, J.; Wei, H.; Wolf, R. M.; Wu, X.; Xiao, L.; York, D. M.; Kollman, P. A., AMBER 18. *Unversity of California, San Francisco* **2018**.
97. Jorgensen, W. L. Chandrasekhar, J.; Madura, J. D.; Impey, R. W.; Klein, M. L.,, Comparison of simple potential functions for simulating liquid water. *J. Chem. Phys.* **1983,** *79*, 926.
98. Maier, J. A. Martinez, C.; Kasavajhala, K.; Wickstrom, L.; Hauser, K. E.; Simmerling, C.,, ff14SBL: improving the accuracy of protein side chain and backbone parameters from ff99SB. *J. Chem. Theory Comput.* **2015,** *11*, 3696.
99. Wang, J. M. Wolf, R. M.; Caldwell, J. W.; Kollman, P. A.; Case, D. A.,, Development and testing of a general amber force field. *J. Comput. Chem.* **2004,** *25*, 1157.
100. Vanquelef, E. Simons, S.; Marquant, G.; Garcia, E.; Klimerak, G.; Delepine, J. C.; Cieplak, P.; Dupradeau, F.-Y.,, R.E.D. Server: a web service for deriving RESP and ESP charges and building force field libraries for new molecules and molecular fragments. . *Nucleic Acids Res.* **2011,** *39*, W511.
101. Cornell, W. D. Cieplak, P.; Bayly, C. I.; Kollman, P. A.,, Application of RESP charges to calculate conformational energies, hydrogen bond energies, and free energies of solvation. *J. Am. Chem. Soc.* **1993,** *115*, 9620.
102. Frisch, M. J. Trucks, G. W.; Schlegel, H. B.; Scuseria, G. E.; Robb, M. A.; Cheeseman, J. R.; Scalmani, G.; Barone, V.; Mennucci, B.; Petersson, G. A.; Nakatsuji, H.; Caricato, M.; Li, X.; Hratchian, H. P.; Izmaylov, A. F.; Bloino, J.; Zheng, G.; Sonnenberg, J. L.; Hada, M.; Ehara, M.; Toyota, K.; Fukuda, R.; Hasegawa, J.; Ishida, M.; Nakajima, T.; Honda, Y.; Kitao, O.; Nakai, H.; Vreven, T.; Montgomery, J. J. A.; Peralta, J. E.; Ogliaro, F.; Bearpark, M.; Heyd, J. J.; Brothers, E.; Kudin, K. N.; Staroverov, V. N.; Kobayashi, R.; Normand, J.; Raghavachari, K.; Rendell, A.; Burant, J. C.; Iyengar, S. S.; Tomasi, J.; Cossi,

M.; Rega, N.; Millam, N. J.; Klene, M.; Knox, J. E.; Cross, J. B.; Bakken, V.; Adamo, C.; Jaramillo, J.; Gomperts, R.; Stratmann, R. E.; Yazyev, O.; Austin, A. J.; Cammi, R.; Pomelli, C.; Ochterski, J. W.; Martin, R. L.; Morokuma, K.; Zakrzewski, V. G.; Voth, G. A.; Salvador, P.; Dannenberg, J. J.; Dapprich, S.; Daniels, A. D.; Farkas, Ö.; Foresman, J. B.; Ortiz, J. V.; Cioslowski, J.; Fox, D. J., Gaussian 09, Revision B.1. *Gaussian, Inc.; Wallingford CT* **2009**.

103. Ryckaert, J. P. Ciccotti, G.; Berendsen, H. J. C., Numerical integration of the Cartesian equations of motion of a system with constraints: molecular dynamics of n-alkanes. *J. Comput. Phys.* **1977,** *23*, 327.

104. Darden, T. York, D.; Pedersen, L., Particle mesh Ewald: an N•log(N) method for Ewald sums in large systems. *J. Chem. Phys.* **1993,** *98*, 10089.

105. Izaguirre, J. A. Catarello, D. P.; Wozniak, J. M.; Skeel, R. D., Langevin stabilization of molecular dynamics. *J. Chem. Phys.* **2001,** *114*, 2090.

106. Berendsen, H. J. C. Postma, J. P. M.; Vangunsteren, W. F.; Dinola, A.; Haak, J. R., Molecular dynamics with coupling to an external bath. *J. Chem. Phys.* **1984,** *81*, 3684.

107. Srinivasan, J. Cheatham, T. E.; Cieplak, P.; Kollman, P. A.; Case, D. A., Continuum solvent studies of the stability of DNA, RNA, and phosphoramidate-DNA helices. *J. Am. Chem. Soc.* **1998,** *120*, 9401.

108. Luo, R. David, L.; Gilson, M. K., Accelerated Poisson-Boltzmann calculations for static and dynamic systems. *J. Comput. Chem.* **2002,** *23*, 1244.

109. Onufriev, A. Bashford, D.; Case, D. A., Exploring protein native states and large-scale conformational changes with a modified generalized Born model. *Proteins: Struct. Funct. Bioinform.* **2004,** *55*, 383.

110. Connolly, M. L., Analytical molecular surface calculation. *J. Appl. Crystallogr.* **1983,** *16*, 548.

111. Feig, M. Karanicolas, J.; Brooks, C. L., MMTSB Tool Set: enhanced sampling and multiscale modeling methods for applications in structural biology. *J. Mol. Graphics Model.* **2004,** *22*, 377.

112. Karpen, M. E. Tobias, D. J.; Brooks, C. L., Statistical clustering techniques for the analysis of long molecular dynamics trajectories: analysis of 2.2-ns trajectories of YPGDV. *Biochemistry* **1993,** *32*, 412.

113. Carpenter, G. A. Grossberg, S., ART-2: self-organisation of stable category recognition codes for analog input patterns. *Appl. Opt.* **1987,** *26*, 4919.